Permeability characterization of ferrites in the radio frequency range

Author: Mireia Alenyà Sistané

Advisor: Arturo Lousa Rodríguez

Facultat de Física, Universitat de Barcelona, Diagonal 645, 08028 Barcelona, Spain*.

Abstract: Soft ferrites are employed in applications from the kHz to the GHz frequency range due to its high magnetic saturation, low coercivity fields and high electrical resistivity. Measuring the complex magnetic permeability in the range from low frequencies to the radio frequency may be performed using two complementary techniques: impedance spectroscopy and coaxial transmission line. The procedures to extract the real dependence of the permeability from the experimental measurements are presented. The experimental permeability of three different ferrites are presented and modelled considering two sources of dispersion: the spin rotational magnetization and the domain wall motion. A good fit of the experimental results is obtained for ferrites that display only one dispersion mechanism after applying the required corrections of stray capacitance, Skin effect and electrical conductivity. For the ferrite showing the two magnetization processes, only a rough adjust has been achieved, although it is shown to be comparable to the ones reported in the recent scientific literature.

I. INTRODUCTION

Ferrites are ferrimagnetic ceramic materials made of oxidized iron and other metals in a brittle ceramic state. They are hard, brittle, and characterized by extremely high electrical resistivity. In terms of their magnetic properties, they can be classified into soft and hard ferrites due to their magnetic coercivity. In particular, soft ferrites present high magnetic saturation and low coercivity fields.

Spinel ferrites are usually described by the formula AB_2O_4 where A and B represent cationic metals, and most of the times one of them is iron. They crystallise in a cubic crystal system with O^{2-} ions placed in one face-centered cubic lattice, with A cations occupying one eighth of the tetrahedral holes and B cations occupying half of the octahedral holes.
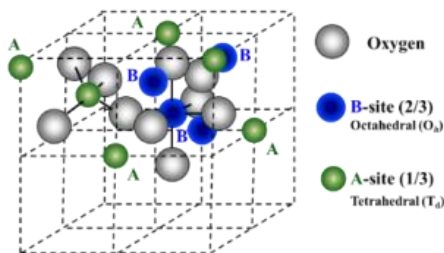

FIG. 1: Ferrite crystal structure

They are widely used in processing electronic signals as inductors (low-noise amplifiers or filters) and for suppressing electromagnetic interferences (EMI). In addition, they are used in high frequency applications because they are not limited by Skin effect (telecommunications or microwave technology), and in power applications because they are able to prevent Eddy currents in the core due to their high resistivity (computers, all kind of peripherals, TV and video systems) [1].

Ferrite cores are fabricated by two basic steps, which are milling and sintering. [2] First, ceramic compounds are milled into particles smaller than 2 μm, small enough that each particle consists of a one single magnetic domain. Then ferrite is obtained by dry pressing and sintering the material above 10 tons per surface square inch. The complex permeability spectra of ferrites not only depends on the chemical composition but also on microstructure such as grain size, porosity or density. Those parameters will also define, for example, the value of electrical losses, permeability and core density. Otherwise, because of the current tendency to circuit miniaturization, ferrites are also prepared as thin films and as nanostructured materials.

Therefore, ferrite is a compound of little compacted crystal grains. Every crystal is a magnetic domain so in its region there is a local saturated magnetization. Domain walls separate these uniform magnetized zones from each other.

Without applying any magnetic field, the domains are randomly oriented allowing the system to have the state of less potential energy. In this situation, the total magnetization is zero. Applying weak fields, the magnetization tends to get oriented towards the magnetic field, so domain walls change their distribution creating new bigger domains generating net magnetizations, which can be extremely high. According to these phenomena, magnetic permeability in range of 100000 can be achieved [3]. If in this situation magnetic field is supressed, magnetic domains return to their magnetic neutral position by a relaxation process.

In this work, we present the results of the measurement of the complex permeability of one ferrite material in the range of 5 Hz – 13 MHz done in our Laboratory. Besides, we also present the results of two other ferrites obtained from several scientific papers. These experimental results are discussed in the frame of the magnetic models for the dependence of the ferrites permeability with frequency.

II. DISPERSION MODEL

It is known that the complex permeability is composed of two different magnetization mechanisms and those are the spin rotational magnetization and the domain wall motion. The first one is a relaxation type factor and its dispersion is inversely proportional to frequency. Otherwise, the domain wall contribution is of resonance type and depends on the square of the frequency. [4]

---

* Electronic address: `malenysi7@alumnes.ub.edu`

The general expression of the permeability is:

$$\hat{\mu}(\omega) = 1 + \hat{\chi}_{sp}(\omega) + \hat{\chi}_{dw}(\omega) \qquad (1)$$

Assuming that each component can be described as a single process, they can be written as:

$$\hat{\chi}_{sp}(\omega) = \frac{\chi_{sp}^0}{1 + j\left(\frac{\omega}{\omega_{sp}}\right)}$$

$$\hat{\chi}_{dw}(\omega) = \frac{\chi_{sp}^0}{1 - \left(\frac{\omega}{\omega_{dw}}\right)^2 + j\left(\frac{\beta}{\omega_{dw}}\right)\left(\frac{\omega}{\omega_{dw}}\right)} \qquad (2)$$

where ω is the frequency, χ_{sp}^0 and χ_{dw}^0 are the static susceptibilities of the spin resonance and domain wall motion, τ is the relaxation time of spin rotational magnetization ($\omega_{sp} \equiv 1/\tau$), ω_{dw} is the resonance frequency and β is the frictional damping coefficient of the domain wall motion.

The first formula corresponds to a Debye equation in which the damping friction is supposed to be large enough to be neglected. It means that after applying a step signal, the dipolar magnetization evolves exponentially in time with a relaxation time τ.

The second equation is of Lorentz type and corresponds to a resonant behaviour of susceptibility, characterized by a resonance frequency ω_{dw} and a damping factor β.

Usually, there is a relevant interplay between the resonance due to the domain wall motion and relaxation due to the spin rotation. Then, it is very difficult to distinguish the weight of each contribution to the permeability dispersion as well as to specify precisely the frequency at which each process takes place [5]. On the other hand, it has been pointed out that the domain wall resonance frequency is commonly lower than the relaxation of the spin rotation magnetization [6].

III. EXPERIMENTAL

Measurements of magnetic permeability were done using the impedance analyser HP 4192A between 5 Hz – 13 MHz. By applying for each frequency one alternating voltage with constant amplitude of 1 V, the system measures the in-phase and in quadrature components of the current. From these parameters, it calculates the real and imaginary parts of the complex impedance.

The experimental measurements were done using a toroidal-shaped ferrite core type T150 (FIG. 2) with complex permeability:

$$\mu(\omega) = \mu'(\omega) - j\,\mu''(\omega) \qquad (3)$$

where μ' and μ'' are the real and imaginary parts of permeability.

FIG. 2: Measured ferrite T150.

The toroid geometric dimensions were: inner diameter $d_1 = 13.8$ mm, outer diameter $d_2 = 27$ mm and thickness $h = 5.6$ mm. The wire winding was of N = 9 turns with a wire thickness $\Phi = 0.6$ mm. A scheme of the toroid winding and the ideal equivalent circuit of such a toroid is presented in FIG. 3b.
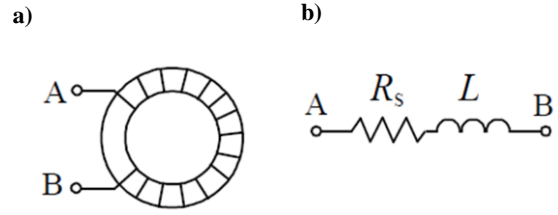

FIG. 3: **a)** Ferrite core with windings; **b)** ideal equivalent circuit considering only series resistance and inductance.

The value R_s represents the resistance of the copper wire and L is the complex inductance that can be written as:

$$\hat{L}(\omega) = L'(\omega) - jL''(\omega)$$

$$\hat{L}(\omega) = L_0 \cdot [\mu_r'(\omega) - j\,\mu_r''(\omega)] \qquad (4)$$

being L_0 the inductance of the toroid without ferrite inside:

$$L_0 = \frac{\mu_0 N^2 d}{2\pi} \cdot \ln\left(\frac{b}{a}\right) \qquad (5)$$

The relation between the measured impedance and R_s and L of the sample is:

$$R_s + j\omega\hat{L} = Z' + j\,Z'' \qquad (6)$$

Once the complex impedance is known, the value of each component of complex permeability is deduced from:

$$\mu_r'(\omega) = \frac{L'(\omega)}{L_0} = \frac{Z''(\omega)}{\omega}$$

$$\mu_r''(\omega) = \frac{L''(\omega)}{L_0} = \frac{Z'(\omega) - R_s}{\omega} \qquad (7)$$

At higher frequencies ($10^7 - 10^{10}$ Hz) other methods like transmission coaxial line technique are used for measuring the complex permeability. This method measures the reflection coefficient,

$$\hat{\Gamma} = \Gamma' - j\Gamma'' \qquad (8)$$

and from its real and imaginary part, complex permeability dependence with frequency is deduced [7].

The toroid shaped sample is placed coaxially inside of a transmission line sector cell ended in short circuit. Magnetic properties can be well measured on these conditions because the system produces a minimum electric field but maximum magnetic field near the sample. The system is shown in FIG. 4.
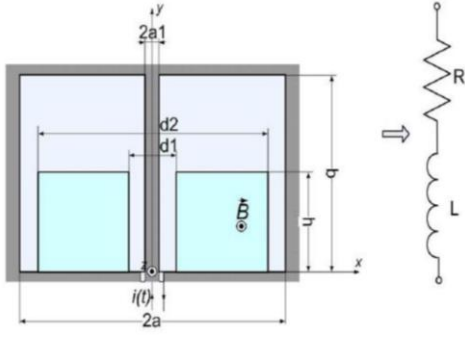
FIG. 4: Cross section of a sample holder with toroidal sample

As the resistance of the cell walls is negligible, the cell impedance is

$$\hat{Z} = j\hat{L}\omega \qquad (9)$$

For the cell of FIG. 4, a simple calculation using the Ampere Theorem leads to:

$$\hat{L} = \frac{\mu_0}{2\pi}\left[(\hat{\mu}_r - 1)h \ln\left(\frac{d_2}{d_1}\right) + b \ln\left(\frac{a}{a_1}\right)\right] \qquad (10)$$

where the cell parameters are a and a_1 the outer and inner radius, and b is its height.

From the experimental values of $\hat{\Gamma}$, the complex impedance can be deduced from:

$$\hat{Z}_{in} = Z_0 \frac{1 + \hat{\Gamma}}{1 - \hat{\Gamma}} \qquad (11)$$

Finally, the complex magnetic permeability value can be obtained from (8) and (9).

IV.   RESULTS AND DISCUSSION

A.   Ferrite B

FIG. 5 shows the theoretical fit of the complex permeability of a ferrite that follows the Debye model. (Data obtained from the literature). This behaviour corresponds to the presence of a single relaxation time. It can be deduced from the maximum of the imaginary part of the complex permeability, which is located exactly in $1/\tau$ where the imaginary part of permeability has a maximum. Furthermore, the Cole-Cole diagram (FIG. 5b) fits in the experimental data as a perfect semi circumference. The fitting parameters are shown on Table I.

The deviation of the imaginary part of permeability at lower frequencies from the Debye model can be explained with a conductivity contribution. For fitting correctly the experimental data, the model must include an additional factor, which is presented in equation (12):

$$\mu_r'^* = \mu_r' - \mu_r'' \cdot \frac{\sigma}{\omega\varepsilon}$$
$$\mu_r''^* = \mu_r'' + \mu_r' \cdot \frac{\sigma}{\omega\varepsilon} \qquad (12)$$

being ε the absolute permittivity of the medium and σ its conductivity.

Although the theory predicts two contributions, only one magnetization process is accessible in this case. The fact that the value of permeability μ_{inf} results 580, suggests that a second process must appear at higher frequencies, which will account of the expected value of 1 for the limit of permeability at very high frequencies. Unfortunately, the lack of experimental data in this range does not allow us to confirm this.

Taking into account that the analysed relaxation occurs at low frequencies we can attribute it to the spin rotational magnetization. The fact that the process is clearly of relaxation type can be explained as due to a large enough damping factor, which will make the resonant process to degenerate in a relaxation type one.
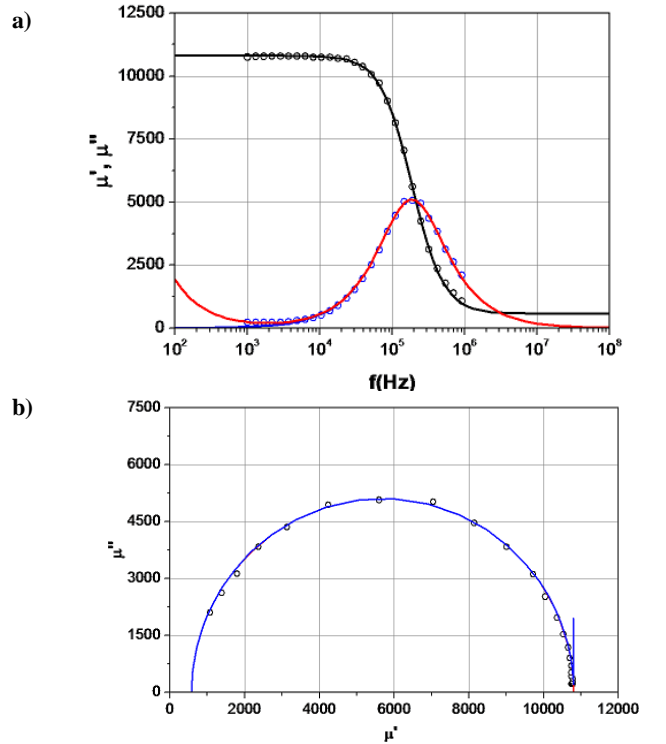

FIG. 5: Experimental data is plotted in open circles and the model in a solid line (the red line considers conductivity); **a)** real and imaginary parts of ferrite B. **b)** Cole-Cole graph.
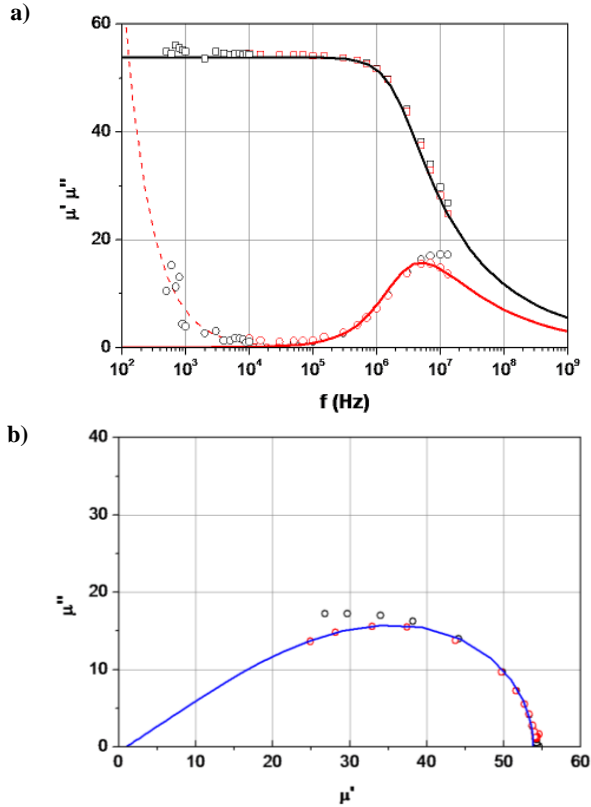
B.   Ferrite T150

The experimental dependence on frequency of the magnetic permeability of Ferrite T150 is shown in FIG. 6a (Data obtained from the literature). It clearly corresponds to a relaxation process. Nevertheless, the asymmetric broadening that shows the magnetic loss peak and the deviation from the circular shape in the Cole-Cole diagram (FIG. 6b) indicates that the relaxation process is not Debye type. The experimental data were adjusted with a Davison Cole model, which is a modification of the Debye model (first equation in (2)) in which the denominator is raised to the power (1-n), and n value is comprised between 0 and 1. The result is shown in FIG. 6b and the fitting parameters are listed in Table I.

It is worth noting here that some correction factors have been considered in order to fit in the experimental data. The first one is the intrinsic resistance R_0 of the copper wire, and this value has been obtained with a lineal regression of the

experimental impedance at low frequencies. The corrected impedance data, knowing that $R_0 = (0.006 \pm 0.001)\ \Omega$, is turned into:

$$\hat{Z}_{cor}^{R_0} = \hat{Z}_{exp} - R_0 \qquad (13)$$

Another factor that could cause a deviation of the experimental data from the model is the Skin effect in the copper wire. Its calculated contribution has been of the order of 10^{-3}-10^{-4}, only a 1% of the experimental permeability value in the most extreme case. Consequently, the weight of this effect can be neglected.

FIG. 6: **a)** Real and imaginary parts of permeability behaviour with frequency for Ferrite T150; **b)** Davison-Cole graph. Black open circles set the experimental data obtained in our Laboratory; red open circles include the stray capacitance correction and solid and dashed lines plot the fit of theoretical model to the corrected data.

The last studied correction is the effect of the stray capacitance of the coil C_p associated to the density of turns of the wire around the ferrite core. The equivalent circuit is now the one presented in FIG. 3b, but with a parallel stray capacitance. According to this, the experimental data can be written as:

$$\frac{1}{\hat{Z}_{exp}} = \frac{1}{\hat{Z}_{coil}} + \frac{1}{\hat{Z}_{C_p}} = \frac{1}{\hat{Z}_{coil}} + jC_p\omega \qquad (14)$$

The applied correction is:

$$\frac{1}{\hat{Z}_{coil}} = \frac{1}{\hat{Z}_{exp}} - jC_p\omega \qquad (15)$$

The stray capacitance value obtained is $C_p = 1$ pF, and after applying this correction, the imaginary part of permeability at high frequencies fits in the modified model.

Ferrite	μ_{est}	μ_{inf}	τ (s)	σ/ε_r (S m^{-1})	n
B	10725	580	$8.5 \cdot 10^{-7}$	$1 \cdot 10^{-9}$	0
H150	53.8	1	$6.9 \cdot 10^{-8}$	$7 \cdot 10^{-9}$	0.625

TABLE I: Fitting parameters of ferrites B and T150.

The asymmetry of the magnetic loss peak can be interpreted as due to an asymmetric distribution of relaxation times, associated to a non-uniform distribution of grain size. Then, while the domains are under the radiofrequency signal, the interplay between them is inhomogeneous, producing a not uniform distribution of relaxation times.

C. Ferrite H40

The complex permeability spectrum of Ferrite H40 (FIG. 7) is more complex than the two previously studied. The real part of magnetic permeability (FIG. 7a) shows a maximum that can be explained by the presence of a resonant magnetization process. Moreover, the imaginary part shows a weak but clear shoulder that suggests that it is composed of two dispersion mechanisms. In addition, this fact gets more evident in the Cole-Cole graph (FIG. 7b), which shows two resonant contributions.
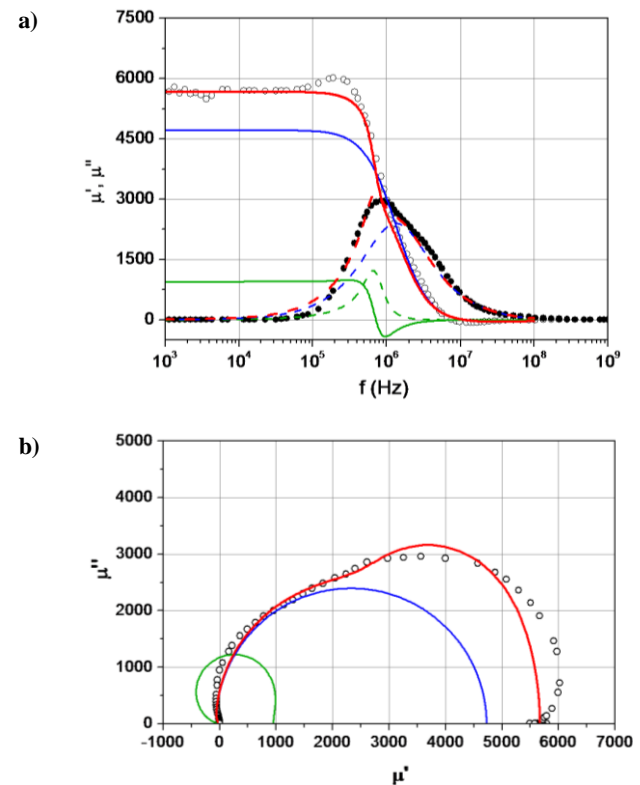
FIG. 7: **a)** Real and imaginary part of permeability dependence with frequency; **b)** Cole-Cole diagram showing the two contributions of magnetization processes, their combination and the experimental data. Experimental values are plotted with open circles, and lines show the total calculated permeability (red) which is make up by spin rotational and domain wall motion components (blue-green).

A model including two magnetization processes is needed to fit in the experimental data. The best fit is present in FIG. 7 with a small resonant contribution at low frequencies that can be attributed to the domain wall motion, and a more relevant relaxation contribution at higher frequencies associated to the spin rotational relaxation. The Cole-Cole graph shows separately both contributions. The fitting parameters are shown in Table II.

Even though we have not achieved a fully satisfactory fitting of the experimental data, our results agree with the general tendency that shows that the frequency of the domain wall motion is usually located at lower frequencies than the spin rotational relaxation frequency [6]. On the other hand, the quality of our fitting is comparable with the one presented by Nakamura [4] which is shown in FIG. 8.
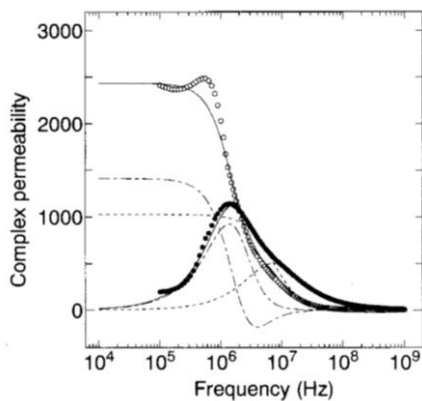

FIG. 8: Complex permeability dependence with frequency of a $Ni_{0.3} Zn_{0.7} Fe_2O_4$ ferrite (From ref [4]).

Ferrite:	Ref. [4]	H40
μ^0_{dw}	1025	950
ω_{dw} (MHz)	7.26	4.50
β (MHz)	4.5	3.6
μ^0_{sp}	1410	4730
τ_{sp} (ns)	433	120
ω_{sp} (MHz)	2.31	9.11

TABLE II: Fitting parameters of a $Ni_{0.3} Zn_{0.7} Fe_2O_4$ ferrite from [4] and ferrite H40.

A more sophisticated model including distributions of resonance frequencies and relaxation times would be necessary for a good fit of the experimental results. Our results should be interpreted as a semi-quantitative approach.

V. CONCLUSIONS

The experimental complex permeability of a commercial T150 ferrite was successfully measured in the range of $10^3 – 1.3 \times 10^7$ Hz using an impedance analyser. Three possible corrections were studied in order to extract the real dependence of the complex permeability. The Skin effect correction was found to be negligible in the whole range of the studied frequencies, while the electrical conductivity was important in the limit of low frequencies and the stray capacitance was important in the limit of high frequencies.

The experimental permeability of three ferrites was characterized according to different models. One of them (Ferrite B) fitted in the Debye model corresponding to a relaxation process of the magnetization with a single relaxation time. A second one (Ferrite T150) was fitted using the Davison-Cole model revealing the presence of an asymmetric distribution of relaxation times, which can be explained assuming one irregular distribution of ferrite grain sizes. Finally, the ferrite H40 shows a more complex spectra with two magnetization processes: a resonant one due to domain wall motion and one more relevant relaxation process due to spin rotation which is dominant at higher frequencies.

---

[1] R. Valenzuela, «*Novel Applications of Ferrites*,» Physics Research International, Vol. 2012, pp. 27-40, 2011.

[2] G. Schaller, «*Ferrite Processing & Effects on Material Performance*,» Ceramic Magnetics, Inc. 16 Law Drive, Fairfield, New Jersey, USA: s.n. 87-90.

[3] N. Hamilton, «*The small-signal frequency Response of Ferrites*,» High Frequency electronics, Vol. 10, 2011.

[4] T. Nakamura, «*Snoek's limit in high-frequency permeability of polycrystalline Ni-Zn, Mg-Zn, and Ni-Zn-Cu spinel ferrites*,» Journal of Applied Physics., Vol. 88, pp. 139-353, 2000.

[5] A. Grusková et al, «*Microwave properties of some substituted LiZn ferrites*,» Journal of Magnetism and Magnetic Materials, Vol. 320, pp. 860-864, 2008.

[6] J. Xie et al, «*Microwave-absorbing properties of NiCoZn spinel ferrites*,» Journal of Magnetism and Magnetic Materials, Vol. 314, pp. 37-42, 2007.

[7] R. Dosoudil et al, «*Computer controlled system for complex permeability measurement in the frequency range of 5 Hz – 1 GHz*,» Journal of Electrical Engineering, Vol 57. NO 8/S, pp. 105-109, 2006.